 CMES, vol.15, no.3, pp.137-146, 2006

Performance of Multiquadric Collocation Method in Solving Lid-driven Cavity Flow Problem with Low Reynolds Number

S. Chantasiriwan[1]

Abstract: The multiquadric collocation method is the collocation method based on radial basis function known as multiquadrics. It has been successfully used to solve several linear and nonlinear problems. Although fluid flow problems are among problems previously solved by this method, there is still an outstanding issue regarding the influence of the free parameter of multiquadrics (or the shape parameter) on the performance of the method. This paper provides additional results of using the multiquadric collocation method to solve the lid-driven cavity flow problem. The method is used to solve the problem in the stream function-vorticity formulation and the velocity-vorticity formulation. Two test problems are solved, and solutions are compared with exact and benchmark solutions. It is found that the shape parameter affects solutions for the stream function-vorticity formulation differently from solutions for the velocity-vorticity formulation.

keyword: Navier-Stokes, Meshless, Multiquadrics, Radial basis function

1 Introduction

Conventional numerical methods like the finite element method and the finite difference method require either time-consuming mesh generation or restrictive node arrangement. Meshless methods have been given much interest recently because they do not have such disadvantages. One popular meshless method is the meshless local Petrov-Garlerkin method (MLPG). This method has been used to solve elastostatic problems [Vavourakis, Sellountos, and Polyzos (2006); Sellountos, Vavourakis, and Polyzos (2005); Atluri, Han, and Rajendran (2004); Han and Atluri (2004)], thermomechanic problems [Ching and Chen (2006)], bending problems of shear deformable shallow shells [Sladek, Sladek, Wen, and Aliabadi (2006)], dynamics fracture problems [Gao, Liu, and Liu (2006)], nonlinear problems with large deformations and rotations [Han, Rajendran, and Atluri (2005)]. In addition, MLPG has also been successfully used in modeling liquid crystals [Pecher, Elston, and Raynes (2006)], simulations of water waves [Ma (2005)], studying vibrations of cracked Euler-Bernoulli beams [Andreaus, Batra, and Porfiri (2005)], multiscale simulations [Shen and Atluri (2005); Shen and Atluri (2004)], and analysis of thick plates [Soric, Li, Jarak, and Atluri (2004)].

Whereas some meshless methods like MLPG seek weak-form solutions, other meshless methods seek strong-form solutions. One such method is the collocation method using radial basis functions. A radial basis function is a function that depends on only the distance between the point where the function is to be evaluated and the center of the function. Radial basis functions have been extensively used in numerical analysis. Examples of applications of radial basis functions are optimization problems [Lian and Liou (2005); Wang and Wang (2006)], fluid-structure interaction problems [Ahrem, Beckert, and Wendland (2006)], mathematical finance problems [Choi and Marcozzi (2004)], analysis of micro-electrical-mechanical system [Hon, Ling, and Liew (2005)], and approximation of source term in dual reciprocity method [Cho, Golberg, Muleshkov, and Li (2004)].

A well-known radial basis function is multiquadrics:

$$\phi(x,y,x_j,y_j) = \sqrt{(x-x_j)^2+(y-y_j)^2+c^2} \tag{1}$$

where (x_j, y_j) is the center of the function. Introduced by Hardy (1971) for the purpose of multivariate data fitting, multiquadrics was later found by Kansa (1990) to be a good basis function for a collocation method. The collocation method that uses multiquadrics as basis function (to be referred to as the multiquadric collocation method or MCM) has been used to solve a variety of partial differential equations by approximating the dependent variable (or its derivative) as a linear combination of multi-

[1] Faculty of Engineering, Thammasat University, Thailand.

quadrics:

$$f(x,y) = \sum_j a_j \phi(x,y,x_j,y_j) \tag{2}$$

Coefficients a_j are determined from the governing equation, the intial condition, and the boundary condition.

A distinctive feature of MCM is the adjustable free parameter (c), which is also known as the shape parameter. Previous experiences obtained from using MCM to solve linear partial differential equations have shown that the accuracy of this method can be increased by increasing the shape parameter. Although there is a practical limit to the acceptable value of the shape parameter due to the large condition number of the system of linear algebraic equations resulting from discretization or the sensitivity of solution to uncertainty in boundary condition as shown by Chantasiriwan (2005), it is generally accepted that the influence of the shape parameter on solutions to linear problems by MCM is more or less predictable.

Recently, there have been attempts to use MCM to solve more challenging problems. One such problem is the lid-driven cavity flow problem. In this paper, this problem means an internal flow of an incompressible, viscous, Newtonian fluid in a square cavity, of which three sides are stationary and the remaining side moves at a constant velocity. Figure 1 illustrates the geometry of this flow problem. Although it can be seen that the lid-driven cavity flow problem looks simple, analytical solutions for this problem are not available except for the case of Stokes flow, in which the fluid viscosity is infinite or the lid speed is infinitesimal. However, benchmark numerical solutions for this problem are available in some cases. This problem is, therefore, a favorite test problem for numerical methods.

Previous results have shown that MCM is capable of providing accurate solution when the shape parameter has particular values. It is unreasonable to assume that influences of the shape parameter on the solution of lid-driven cavity flow problem and a linear problem are similar. Two differences must be considered. First, the nonlinearity of the lid-driven cavity flow problem means that not only is the accuracy of the solution is important, the ability of MCM to deliver converged solutions must also be paid attention to. There is no doubt that the value of the shape parameter plays a strong role in determining whether MCM converges. Second, boundary condition of the problem is discontinuous whereas most previous results that show predictable behaviors of solutions by MCM have been obtained from test problems having continuous boundary conditions. Unfortunately, the effect of the shape parameter on the performance of MCM in the lid-driven cavity flow problem has not been sufficiently investigated.

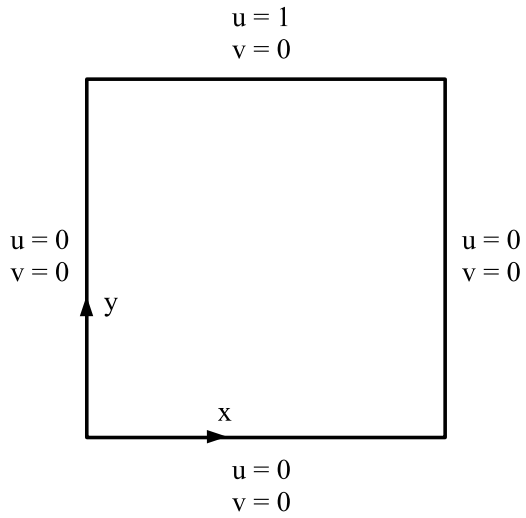

Figure 1 : Lid-driven flow in a square cavity

This paper seeks to provide additional results of using MCM to solve the lid-driven cavity flow problem. The main issue of concern is the influence of the shape parameter on the accuracy of the solution and the number of iterations required for convergence. These results will be useful for practical purpose of determining the suitable range of the values of the shape parameter so that MCM can be used with confidence. The following sections present mathematical formulations of the problem, description of MCM used to solve the problem, details of two test problems along their exact and benchmark solutions for computing errors of MCM, and results of using MCM to solve the test problems.

2 Test problems

Two test problems are considered. The first problem is the Stokes problem (Re = 0), and the second problem is a low-Re problem (Re = 100). The first problem is a linear problem for which the analytical solution is available, whereas the second problem is a nonlinear problem without the exact solution. However, a widely accepted benchmark solution is available for the second problem.

Both solutions can be used to assess the accuracy of a numerical method.

For the first problem, an eigenfunction expansion procedure is used to express the analytical solution as an infinite series. Eigenvalues are computed by using an iteration method suggested by Hansen (1997). Coefficients of expansion are determined numerically by using a method based on a least-square procedure suggested by Shankar (1993). Table 1 shows solution obtained from truncated series having 1000 terms at selected points inside the cavity. Also shown in Tab. 1 is benchmark solution at the selected points for the second problem provided by Ghia, Ghia, and Shin (1982).

Table 1 : Analytical solution for the first test problem (Re = 0) and benchmark solution for the second test problem (Re = 100) at selected points inside the cavity

x	y	Re = 0	Re = 100
		u	
0.5	0.9766	0.86477	0.84123
0.5	0.9688	0.82077	0.78871
0.5	0.9609	0.77685	0.73722
0.5	0.9531	0.73420	0.68717
0.5	0.8516	0.26154	0.23151
0.5	0.7344	-0.06245	0.00332
0.5	0.6172	-0.18968	-0.13641
0.5	0.5000	-0.20519	-0.20581
0.5	0.4531	-0.19577	-0.21090
0.5	0.2813	-0.13515	-0.15662
0.5	0.1719	-0.09030	-0.10150
0.5	0.1016	-0.05855	-0.06434
0.5	0.0703	-0.04272	-0.04775
0.5	0.0625	-0.03853	-0.04192
0.5	0.0547	-0.03423	-0.03717
x	y	Re = 0	Re = 100
		v	
0.9688	0.5	-0.05096	-0.05906
0.9609	0.5	-0.06272	-0.07391
0.9531	0.5	-0.07385	-0.08864
0.9453	0.5	-0.08447	-0.10313
0.9063	0.5	-0.12965	-0.16914
0.8594	0.5	-0.16581	-0.22445
0.8047	0.5	-0.18370	-0.24533
0.5000	0.5	0	0.05454
0.2344	0.5	0.18228	0.17527
0.2266	0.5	0.18341	0.17507
0.1563	0.5	0.17352	0.16077
0.0938	0.5	0.12975	0.12317
0.0781	0.5	0.11320	0.10890
0.0703	0.5	0.10415	0.10091
0.0625	0.5	0.09457	0.09233

3 Formulations of the problem

The lid-driven cavity flow problem can be solved in three well-known formulations. Their details are given as follows.

1. The primitive-variable formulation yields three equations of pressure and velocity components:

$$u\frac{\partial u}{\partial x}+v\frac{\partial u}{\partial y}=-\frac{\partial p}{\partial x}+\frac{1}{\mathrm{Re}}\left(\frac{\partial^2 u}{\partial x^2}+\frac{\partial^2 u}{\partial y^2}\right) \tag{3}$$

$$u\frac{\partial v}{\partial x}+v\frac{\partial v}{\partial y}=-\frac{\partial p}{\partial y}+\frac{1}{\mathrm{Re}}\left(\frac{\partial^2 v}{\partial x^2}+\frac{\partial^2 v}{\partial y^2}\right) \tag{4}$$

$$\frac{\partial u}{\partial x}+\frac{\partial v}{\partial y}=0 \tag{5}$$

   Popular methods for solving the Navier-Stokes equations in this formulation are mesh-dependent methods such as the finite difference method, the finite element method, and the finite volume method. Few collocation methods based on radial basis functions have been used to solve the lid-driven cavity flow problem in this formulation. Sarler (2005) solved natural convection problem using a collocation method based on radial basis functions. Ding, Shu, Yeo, and Xu (2006) used local multiquadric collocation method to solve the three-dimensional lid-driven cavity flow problem. Instead of approximating an dependent variable as a linear combination of multiquadrics centered at all nodes like the "global" multiquadric collocation method proposed by Kansa (1990), they approximated the dependent variable using a few support nodes located near the location where the dependent variable was to be determined. This approximation was then used in the differential quadrature algorithm to approximate derivatives of the dependent variable as a weighted sum of values of dependent variables at the support nodes.

2. The velocity-vorticity formulation provides three

equations of vorticity and velocity components:

$$\frac{\partial^2\omega}{\partial x^2}+\frac{\partial^2\omega}{\partial y^2}=\mathrm{Re}\left(u\frac{\partial\omega}{\partial x}+v\frac{\partial\omega}{\partial y}\right) \tag{6}$$

$$\frac{\partial^2 u}{\partial x^2}+\frac{\partial^2 u}{\partial y^2}=-\frac{\partial\omega}{\partial y} \tag{7}$$

$$\frac{\partial^2 v}{\partial x^2}+\frac{\partial^2 v}{\partial y^2}=\frac{\partial\omega}{\partial x} \tag{8}$$

Young, Lane, Lin, Chiu, and Chen (2004) solved the Stokes flow problem in cavity by the multiquadric collocation method using this formulation.

3. The stream function-vorticity formulation results from making use of the stream function (ψ), from which velocity components can be found ($u=\partial\psi/\partial y$, $v=-\partial\psi/\partial x$). Two equations of stream function and vorticity are

$$\frac{\partial^2\psi}{\partial x^2}+\frac{\partial^2\psi}{\partial y^2}=-\omega \tag{9}$$

$$\frac{\partial^2\omega}{\partial x^2}+\frac{\partial^2\omega}{\partial y^2}=\mathrm{Re}\left(u\frac{\partial\omega}{\partial x}+v\frac{\partial\omega}{\partial y}\right) \tag{10}$$

The local multiquadric collocation method used by Shu, Ding, and Yeo (2005) to solve the lid-driven cavity flow problem in this formulation is similar to the method used by Tolstykh and Shirobokov (2005). Mai-Duy and Tran-Cong (2001) solved the same problem using an "indirect" multiquadric collocation method. Their method differs from the original method [Kansa (1990)] in that derivatives of dependent variables are approximated by linear combinations of multiquadrics. Approximations for dependent variables can be found from integrals of multiquadrics. This method was also successfully used to solve natural convection problem [Mai-Duy (2004)] and transient problems [Mai-Cao and Tran-Cong (2005)].

Equations (9) and (10) can be combined into an equation of stream function:

$$\frac{\partial^4\psi}{\partial x^4}+2\frac{\partial^4\psi}{\partial x^2\partial y^2}+\frac{\partial^4\psi}{\partial x^4} =\mathrm{Re}\left[u\left(\frac{\partial^3\psi}{\partial x^3}+\frac{\partial^3\psi}{\partial x\partial y^2}\right)+v\left(\frac{\partial^3\psi}{\partial x^2\partial y}+\frac{\partial^3\psi}{\partial y^3}\right)\right] \tag{11}$$

Recently, Mai-Duy and Tran-Cong (2006) proposed an indirect multiquadric collocation method for solving the biharmonic equation, which is simply Eq. (11) in the case of Re = 0.

4 Multiquadric collocation method

Assume that there are N collocation nodes, divided into N_b boundary nodes and N_i interior nodes ($N=N_b+N_i$). Let (ξ_1,η_1), (ξ_2,η_2), ..., (ξ_{N_b},η_{N_b}) denote coordinates of boundary nodes, and $(\xi_{N_b+1},\eta_{N_b+1})$, $(\xi_{N_b+2},\eta_{N_b+2})$, ..., (ξ_N,η_N) denote coordinates of interior nodes. These N nodes are uniformly distributed in the domain, forming a square grid with the grid spacing equal to $1/(\sqrt{N}-1)$.

4.1 MCM1

MCM1 solves the problem in the stream function-vorticity formulation. The stream function at the k$^{\mathrm{th}}$ iteration is approximated as

$$\psi^{(k)}(x,y)=\sum_{j=1}^{N}a_j^{(k)}\phi(x,y,\xi_j,\eta_j) \tag{12}$$

Interior nodes are used for discretization of the governing equations, whereas boundary nodes are used for discretization of boundary condtions. For the purpose of iterative determination of N unknown coefficients $a_j^{(k)}$, a_j^* are solved from the governing equation:

$$\frac{\partial^4\psi^*}{\partial x^4}+2\frac{\partial^4\psi^*}{\partial x^2\partial y^2}+\frac{\partial^4\psi^*}{\partial x^4} =\mathrm{Re}\left[u^{(k-1)}\left(\frac{\partial^3\psi^{(k-1)}}{\partial x^3}+\frac{\partial^3\psi^{(k-1)}}{\partial x\partial y^2}\right) + v^{(k-1)}\left(\frac{\partial^3\psi^{(k-1)}}{\partial x^2\partial y}+\frac{\partial^3\psi^{(k-1)}}{\partial y^3}\right)\right] \tag{13}$$

and boundary condition:

$$\frac{\partial\psi^*}{\partial y}=u_\Gamma \tag{14}$$

$$-\frac{\partial\psi^*}{\partial x}=v_\Gamma \tag{15}$$

where u_Γ and v_Γ are velocity components at the boundary of the cavity as shown in Fig. 1. After obtaining a_j^*, $a_j^{(k)}$ are determined from

$$a_j^{(k)}=\theta a_j^*+(1-\theta)a_j^{(k-1)} \tag{16}$$

where θ is the relaxation parameter. Initially, let $a_j^{(0)} = 0$. After each iteration, velocity components at N_t test nodes are computed from

$$u_i^{(k)} = \sum_{j=1}^{N} a_j^{(k)} \frac{\partial \psi}{\partial y}(x_i, y_i, \xi_j, \eta_j) \tag{17}$$

$$v_i^{(k)} = -\sum_{j=1}^{N} a_j^{(k)} \frac{\partial \psi}{\partial x}(x_i, y_i, \xi_j, \eta_j) \tag{18}$$

where (x_i, y_i) are coordinates of test nodes given in Tab. 1. The iteration process is continued until the convergence criteria are satisfied:

$$\sqrt{\frac{\sum_{i=1}^{N_t} \left(f_i^{(k)} - f_i^{(k-1)} \right)^2}{\sum_{i=1}^{N_t} \left(f_i^{(k)} \right)^2}} < 10^{-4} \tag{19}$$

where f denotes either u or v, depending on the test node. (See Tab. 1.) The number of iterations for converged solution is denoted by K. If more than 200 iterations are required, it is considered that no converged solution can be found. Note that, if Re = 0 (Stokes flow), a_j^* obtained from solving Eqs. (13) - (15) are used to determine velocity components without iteration. Once a converged solution has been found, its error may be computed from

$$\varepsilon = \sqrt{\sum_{i=1}^{N_t} \left(f_i^{(k)} - f_{i,\,exact}^{(k-1)} \right)} \tag{20}$$

Table 1 gives $u_{i,\,exact}$ and $v_{i,\,exact}$ at the test nodes.

4.2 MCM2

MCM2 solves the problem in the vorticity-velocity formulation. It is an extension of the method proposed by Young, Lane, Lin, Chiu, and Chen (2004) to solve Stokes flow problem. In this method, vorticity and velocity components are approximated as

$$u^{(k)}(x,y) = \sum_{j=1}^{N} b_j^{(k)} \phi(x, y, \xi_j, \eta_j) \tag{21}$$

$$v^{(k)}(x,y) = \sum_{j=1}^{N} c_j^{(k)} \phi(x, y, \xi_j, \eta_j) \tag{22}$$

$$\omega^{(k)}(x,y) = \sum_{j=1}^{N} d_j^{(k)} \phi(x, y, \xi_j, \eta_j) \tag{23}$$

The k^{th} iteration loop begins by solving the following equation:

$$\frac{\partial^2 u^*}{\partial x^2} + \frac{\partial^2 u^*}{\partial y^2} = -\frac{\partial \omega^{k-1}}{\partial y} \tag{24}$$

along with the boundary condition:

$$u^* = u_\Gamma \tag{25}$$

for b_j^*. Then $b_j^{(k)}$ are determined from

$$b_j^{(k)} = \theta b_j^* + (1-\theta) b_j^{(k-1)} \tag{26}$$

Next, the following equation:

$$\frac{\partial^2 v^*}{\partial x^2} + \frac{\partial^2 v^*}{\partial y^2} = \frac{\partial \omega^{k-1}}{\partial x} \tag{27}$$

is solved along with the boundary condition:

$$v^* = v_\Gamma \tag{28}$$

for c_j^*. Then $c_j^{(k)}$ are determined from

$$c_j^{(k)} = \theta c_j^* + (1-\theta) c_j^{(k-1)} \tag{29}$$

Finally, the following equation:

$$\frac{\partial^2 \omega^*}{\partial x^2} + \frac{\partial^2 \omega^*}{\partial y^2} = \mathrm{Re}\left(u^{(k-1)} \frac{\partial \omega^{(k-1)}}{\partial x} + v^{(k-1)} \frac{\partial \omega^{(k-1)}}{\partial y} \right) \tag{30}$$

is solved along with the boundary condition:

$$\omega^* = \frac{\partial v^*}{\partial x} - \frac{\partial u^*}{\partial y} \tag{31}$$

for d_j^*, Then $d_j^{(k)}$ are determined from

$$d_j^{(k)} = \theta d_j^* + (1-\theta) d_j^{(k-1)} \tag{32}$$

Initially, let $b_j^{(0)}$, $c_j^{(0)}$, $d_j^{(0)} = 0$. The iteration process is continued until the convergence criteria given in Eq. (19) are satisfied. As in the case of MCM1, K denotes the number of iterations required for convergence. It is interesting to note that $K > 1$ even when Re = 0. In other words, iterations are required for solutions of both test problems by MCM2. Error of the solution of MCM2 is also calculated by using Eq. (20).

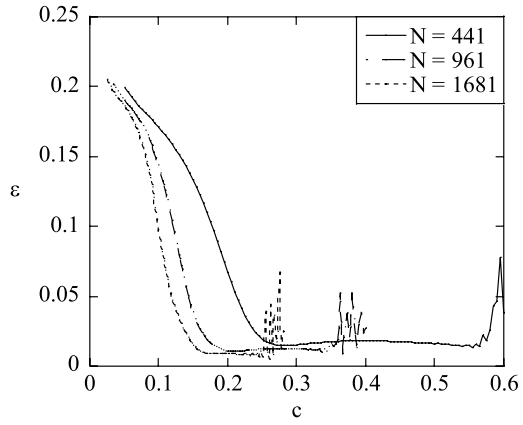

Figure 2 : Variation with the shape parameter of error (ε) of solution to the first test problem by MCM1 for N = 441, 981, and 1681

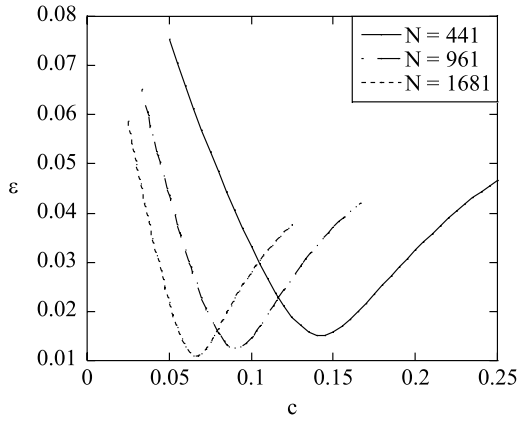

Figure 3 : Variation with the shape parameter of error (ε) of solution to the first test problem by MCM2 for N = 441, 981, and 1681

5 Results and Discussion

5.1 The first test problem (Stokes flow)

Results for MCM1 are shown in Fig. 2. Each curve in Fig. 2 represents the case of a different N. It can be seen that solution is more accurate if N is larger. Notice that each curve in Fig. 2 can be divided into 3 regions. In the first region, ε decreases rapidly as c increases. In the second region, ε is relatively insensitive to c. Increasing N in this region causes the range of c to decrease ($0.25 \leq c \leq 0.5$ for N = 441, $0.2 \leq c \leq 0.3$ for N = 961, and $0.16 \leq c \leq 0.21$ for N = 1681). In the third region, the solution is unstable with respect to c. It is interesting to note that results in Fig. 2 are somewhat different from previous results of using the multiquadric collocation method to solve problems having continuous boundary conditions [Chantasiriwan (2004)], which show that the accuracy for such a problem can be continually increased by increasing c until too large a value of c causes ill-conditioning and round-off errors prevent the solution from being more accurate.

Results for MCM2 are shown in Figs. 3 and 4. A noticeable difference between MCM2 results and MCM1 results is that MCM2 solution is more sensitive to c than MCM1 solution. Minima of the curves in Fig. 3 are easy to locate. They are ε_{min} = 0.0152, 0.0125, 0.0109 at c_{min} = 0.140, 0.090, 0.0675 for N = 441, 961, 1681, respectively. Hence, positions of minima nearly scale with grid spacing. Figure 4 shows that the number of iterations

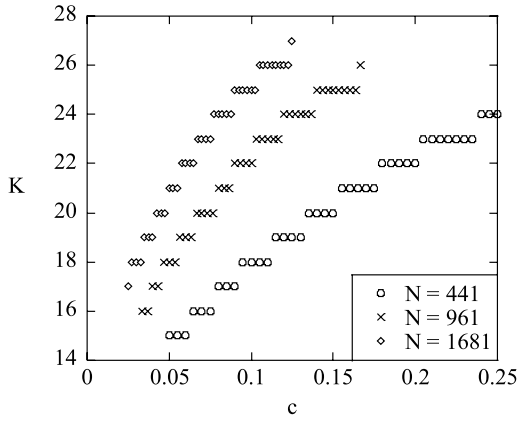

Figure 4 : Variation with the shape parameter of the number of iterations (K) required for converged solution to the first test problem by MCM2 for N = 441, 981, and 1681

required for convergence increases with N and c. The relaxation parameter (θ) is 1 for results in this figure. It is interesting to note that results in Fig. 3 are similar to results of interpolation of rapidly varying functions by multiquadrics [Ling (2004)].

5.2 The second test problem (Flow with Re = 100)

Results for MCM1 are shown in Figs. 5 and 6. Comparison between Figs. 2 and 5 reveals some similarity. However, each curve in Fig. 5 is divided into two sections instead of three sections like each curve in

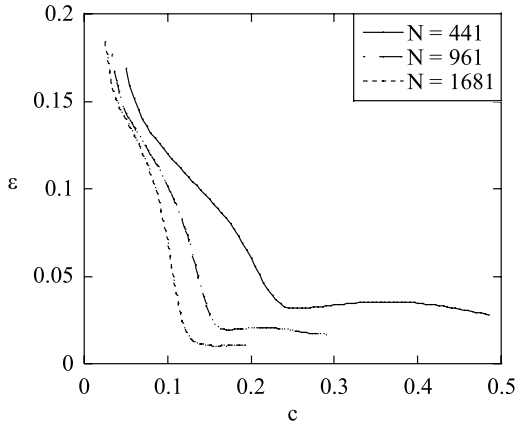

Figure 5 : Variation with the shape parameter of error (ε) of solution to the second test problem by MCM1 for N = 441, 981, and 1681

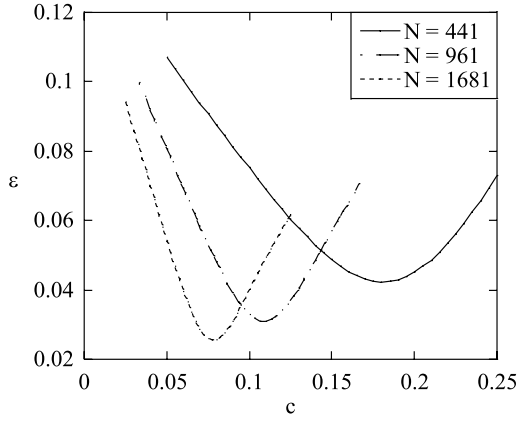

Figure 7 : Variation with the shape parameter of error (ε) of solution to the second test problem by MCM2 for N = 441, 981, and 1681

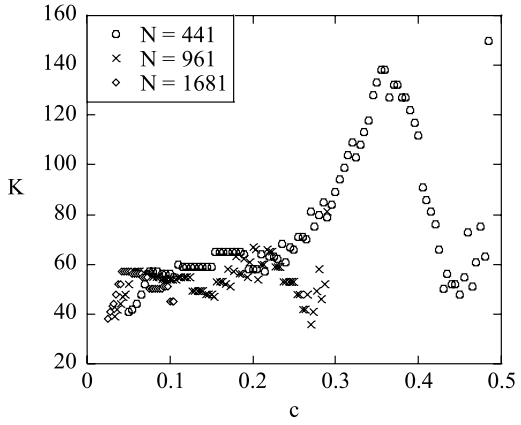

Figure 6 : Variation with the shape parameter of the number of iterations (K) required for converged solution to the second test problem by MCM1 for N = 441, 981, and 1681

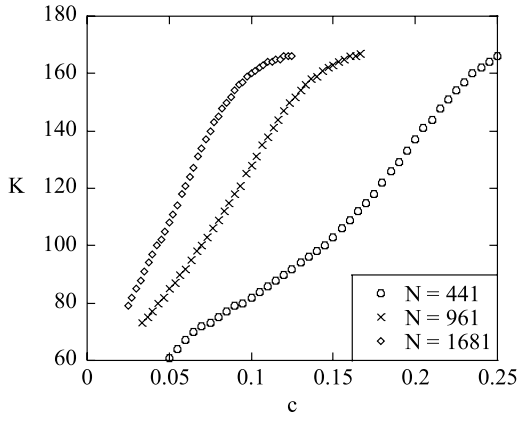

Figure 8 : Variation with the shape parameter of the number of iterations (K) required for converged solution to the second test problem by MCM2 for N = 441, 981, and 1681

Fig. 2. In the first region, ε rapidly decreases as c increases. In the second region, ε is relatively insensitive to c ($0.24 \leq c \leq 0.49$ for N = 441, $0.19 \leq c \leq 0.29$ for N = 961, and $0.14 \leq c \leq 0.21$ for N = 1681). The section of unstable solution does not exist in Fig. 5 because no converged solution can be found if c is too large. Figure 6 show how K varies with c. The relaxation parameter (θ) is 0.2 for results in this figure. It should be noted that there appears to be no discernable pattern of variation of K with c like the pattern found in Fig. 4.

Results for MCM2 are shown in Figs. 7 and 8. It can be seen that MCM2 results for the second test problem and the first test problems behave similarly. In general, solution to the second test problem is less accurate than solution to the first test problem. Minima of the curves in Fig. 7 are = 0.0423, 0.0311, 0.0255 at c_{min} = 0.180, 0.110, 0.0775 for N = 441, 961, 1681, respectively. Figure 8 shows that the number of iterations required for convergence increases with N and c. The relaxation parameter (θ) is 0.2 for results in this figure.

6 Conclusions

The multiquadric collocation method (MCM) is used to solve the lid-driven cavity flow problem in the stream function-vorticity formulation and the velocity-vorticity formulation. This problem is a nonlinear problem with discontinuous boundary condition. It has been found that the accuracy of a solution by MCM to a linear problem with continuous boundary condition increases with the shape parameter of multiquadrics until the shape parameter is large and causes round-off error. Results from this paper indicate that errors of solutions to the lid-driven cavity flow problem by MCM are minimized at optimum values of the shape parameter. Increasing the value of the shape parameter beyond the optimum value results in not only larger error but also more iterations required for convergence. Furthermore, it is found that a solution to the problem in the stream function-vorticity formulation exhibits a range of values of the shape parameter in which the solution is relatively insensitive to the shape parameter. A solution to the problem in the velocity-vorticity formulation is found to be more sensitive to the shape parameter than a solution to the problem in the stream function-vorticity formulation.

Acknowledgement: The author would like to acknowledge the financial support from the Thailand Research Fund.

References

Ahrem, R.; Beckert, A.; Wendland, H. (2006): A meshless spatial coupling scheme for large-scale fluid-structure-interaction problems. *CMES: Computer Modeling in Engineering & Sciences*, vol. 12, pp. 121–136.

Andreaus, U.; Batra, R. C.; Porfiri, M. (2005): Vibrations of cracked Euler-Bernoulli beams using Meshless Local Petrov-Galerkin (MLPG) method. *CMES: Computer Modeling in Engineering & Sciences*, vol. 9, pp. 111–131.

Atluri, S. N.; Han, Z. D.; Rajendran, A. M. (2004): A new implementation of the meshless finite volume method, through the MLPG "mixed" approach. *CMES: Computer Modeling in Engineering & Sciences*, vol. 6, pp. 491–513.

Chantasiriwan, S. (2004): Cartesian grid methods using radial basis functions for solving Poisson, Helmholtz, and diffusion–convection equations. *Engr. Anal. with Bound. Elem.*, vol. 28, pp. 1417–1425.

Chantasiriwan, S. (2005): Solutions of partial differential equations with random Dirichlet boundary conditions by multiquadric collocation method. *Engr. Anal. with Bound. Elem.*, vol. 29, pp. 1124–1129.

Ching, H. K.; Chen, J. K. (2006): Thermomechanical analysis of functionally graded composites under laser heating by the MLPG method. *CMES: Computer Modeling in Engineering & Sciences*, vol. 13, pp. 199–217.

Cho, H. A.; Golberg, M. A.; Muleshkov, A. S.; Li, X. (2004): Trefftz methods for time dependent partial differential equations. *Computers, Materials and Continua*, vol. 1, pp. 1–37.

Choi, S.; Marcozzi, M. D. (2004): On the application of MQ-RBF to the valuation of derivative securities. *CMES: Computer Modeling in Engineering & Sciences*, vol. 5, pp. 201–212.

Ding, H.; Shu, C.; Yeo, K. S.; Xu, D. (2006): Numerical computation of three-dimensional incompressible viscous flows in the primitive variable form by local multiquadric differential quadrature method. *Comp. Meth. Appl. Mech. Engr.*, vol. 195, pp. 516–533.

Gao, L.; Liu, K.; Liu, Y. (2006): Applications of MLPG method in dynamic fracture problems. *CMES: Computer Modeling in Engineering & Sciences*, vol. 12, pp. 181–195.

Ghia, U.; Ghia, K. N.; Shin, C. T. (1982): High-Re solutions for incompressible flow using the Navier-Stokes equations and a multi-grid method. *J. Comp. Phys.*, vol. 48, pp. 387–411.

Han, Z. D.; Atluri, S. N. (2004): Meshless local Petrov-Galerkin (MLPG) approaches for solving 3D problems in elasto-statics. *CMES: Computer Modeling in Engineering & Sciences*, vol. 6, pp. 169–188.

Han, Z. D.; Rajendran, A. M.; Atluri, S. N. (2005): Meshless Local Petrov-Galerkin (MLPG) approaches for solving nonlinear problems with large deformations and rotations. *CMES: Computer Modeling in Engineering & Sciences*, vol. 10, pp. 1–12.

Hansen, E. B. (1997): Root structure and numerical solution of the equation sin z = cz. *Appl. Math. Lett.*, vol. 10, pp. 33–38.

Hardy, R. L. (1971): Multiquadric equation of topography and other irregular surfaces. *J. Geophys. Res.*, vol. 76, pp. 1905–1915.

Hon, Y. C.; Ling, L.; Liew, K. M. (2005): Numerical analysis of parameters in a laminated beam model by radial basis functions. *Computers, Materials and Continua*, vol. 2, pp. 39–49.

Kansa, E. J. (1990): Multiquadrics – a scattered data approximation scheme with applications to computational fluid-dynamics – II solutions to parabolic, hyperbolic and elliptic partial differential equations. *Comp. Math. with Appl.*, vol. 19, pp. 147–161.

Lian, Y. S.; Liou, M. S. (2005): Mining of data from evolutionary algorithms for improving design optimization. *CMES: Computer Modeling in Engineering & Sciences*, vol. 8, pp. 61–72.

Ling, L. (2004): A univariate quasi-multiquadric interpolation with better smoothness. *Comp. Math. with Appl.*, vol. 48, pp. 897–912.

Ma, Q. W. (2005): MLPG method based on Rankine source solution for simulating nonlinear water waves. *CMES: Computer Modeling in Engineering & Sciences*, vol. 9, pp. 193–209.

Mai-Cao, L.; Tran-Cong, T. (2005): A meshless IRBFN-based method for transient problems. *CMES: Computer Modeling in Engineering & Sciences*, vol. 7, pp. 149–171.

Mai-Duy, N. (2004): Indirect RBFN method with scattered points for numerical solution of PDEs. *CMES: Computer Modeling in Engineering & Sciences*, vol. 6, pp. 209–226.

Mai-Duy, N.; Tran-Cong, T. (2001): Numerical solution of Navier-Stokes equations using multiquadric radial basis function networks. *Int. J. Numer. Meth. Fl.*, vol. 37, pp. 65–86.

Mai-Duy, N.; Tran-Cong, T. (2006): Solving biharmonic problems with scattered-point discretization using indirect radial-basis-function networks. *Engr. Anal. with Bound. Elem.*, vol. 30, pp. 77–87.

Pecher, R.; Elston, S.; Raynes, P. (2006): Meshfree solution of Q-tensor equations of nematostatics using the MLPG method. *CMES: Computer Modeling in Engineering & Sciences*, vol. 13, pp. 91–101.

Sarler, B. (2005): A radial basis collocation approach in computational fluid dynamics. *CMES: Computer Modeling in Engineering & Sciences*, vol. 7, pp. 185–193.

Sellountos, E. J.; Vavourakis, V.; Polyzos, D. (2005): A new singular/hypersingular MLPG (LBIE) method for 2D elastostatics. *CMES: Computer Modeling in Engineering & Sciences*, vol. 7, pp. 35–47.

Shankar, P. N. (1993): The eddy structure in Stokes flow in a cavity. *J. Fluid Mech.*, vol. 250, pp. 371–383.

Shen, S.; Atluri, S. N. (2004): Multiscale simulation based on the meshless local Petrov-Galerkin (MLPG) method. *CMES: Computer Modeling in Engineering & Sciences*, vol. 5, pp. 235–255.

Shen, S.; Atluri, S. N. (2005): A tangent stiffness MLPG method for atom/continuum multiscale simulation. *CMES: Computer Modeling in Engineering & Sciences*, vol. 7, pp. 49–67.

Shu, C.; Ding, H.; Yeo, K. S. (2005): Computation of incompressible Navier-Stokes equations by local RBF-based differential quadrature method. *CMES: Computer Modeling in Engineering & Sciences*, vol. 7, pp. 195–205.

Sladek, J.; Sladek, V.; Wen, P. H.; Aliabadi, M. H. (2006): Meshless Local Petrov-Galerkin (MLPG) method for shear deformable shells analysis. *CMES: Computer Modeling in Engineering & Sciences*, vol. 13, pp. 103–117.

Soric, J.; Li, Q.; Jarak, T.; Atluri, S. N. (2004): Meshless Local Petrov-Galerkin (MLPG) formulation for analysis of thick plates. *CMES: Computer Modeling in Engineering & Sciences*, vol. 6, pp. 349–357.

Tolstykh, A. I.; Shirobokov, D. A. (2005): Using radial basis functions in a "finite difference mode". *CMES: Computer Modeling in Engineering & Sciences*, vol. 7, pp. 207–222.

Vavourakis, V.; Sellountos, E. J.; Polyzos, D. (2006): A comparison study on different MLPG (LBIE) formulations. *CMES: Computer Modeling in Engineering & Sciences*, vol. 13, pp. 171–183.

Wang, S. Y.; Wang, M. Y. (2006): Structural shape and topology optimization using an implicit free boundary parametrization method. *CMES: Computer Modeling in Engineering & Sciences*, vol. 13, pp. 119–147.

Young, D. L.; Lane, S. C.; Lin, C. Y.; Chiu, C. L.; Chen, K. C. (2004): Solutions of 2D and 3D Stokes laws using multiquadrics method. *Engr. Anal. with Bound. Elem.*, vol. 28, pp. 1233–1243.